RASĀYAN *J. Chem.*
Vol. 19 | No. 1 | 525-532 | January-March | 2026
ISSN: 0974-1496 | e-ISSN: 0976-0083 | CODEN: RJCABP
http://www.rasayanjournal.com
http://www.rasayanjournal.co.in

EFFECTS OF CITRIC ACID-ASSISTED PH ADJUSTMENT ON THE PURITY AND MORPHOLOGY OF SILICA NANOPARTICLES SYNTHESIZED FROM GEOTHERMAL SLAG

D. C. Birawidha[1,2,✉] A. Manaf [2], W. Astuti[1], A. Daulay[1], H. T. B. Murti Petrus[1,3], U. Dani [4], and S. Widayati[5]

[1]Research Centre for Mineral Technology, National Research and Innovation Agency, Lampung, Indonesia

[2]Department of Physics, Faculty of Mathematics and Natural Sciences, Universitas Indonesia, Depok, Indonesia

[3]Department of Chemical Engineering, Faculty of Engineering, Universitas Gadjah Mada, Yogyakarta, Indonesia

[4]Geological Resource Research Centre, National Research and Innovation Agency, Bandung, Indonesia

[5]Mining Engineering Department, Faculty of Technic, Bandung Islamic University, Bandung, Indonesia

✉Corresponding author: daveok31@gmail.com

ABSTRACT

This study investigates the citric acid-assisted sol-gel synthesis of silica nanoparticles from geothermal slag under microwave heating, with a focus on the effect of pH (1, 3, 5, 7, 13) on product purity, recovery, and morphology. Characterisation via XRF, XRD, FTIR, and FESEM revealed that pH critically determines the synthesis outcome. The highest silica purity (97.494% SiO_2) was achieved at pH 3, whereas maximum recovery (68.94%) occurred at pH 7. Alkaline conditions (pH 13) reduced purity to 84.257% due to metal contamination. FTIR analysis indicated enhanced silanol (Si–OH) formation at pH 3–7, while pH 13 promoted a polymerised Si–O–Si network. Morphological analysis showed homogeneous nanoparticles with a narrower size distribution (80–120 nm) at neutral pH, compared to larger aggregates (150–300 nm) under acidic conditions. These findings demonstrate that pH can be strategically tuned to prioritise either high purity or high yield, providing a scalable and sustainable pathway for valorising geothermal waste into high-value nanomaterials and supporting circular economy objectives.

Keywords: Geothermal Slag, Silica Nanoparticles, Sol-Gel Synthesis, pH Effect, Citric Acid, Microwave Heating, Waste Valorisation.

RASĀYAN *J. Chem.*, Vol. 19, No. 1, 2026

INTRODUCTION

As the world's second-largest geothermal energy producer, Indonesia harnesses a vast renewable resource of 28,617 MW, roughly 40% of global resources.[1] This clean energy source significantly reduces dependence on fossil fuels and greenhouse gas emissions. However, its exploitation presents a persistent technical and environmental challenge: the formation of massive silica scaling. The high silica content in geothermal fluids leads to operational inefficiencies, including pipe blockages and reduced heat transfer, and generates substantial solid waste. For instance, the Dieng Power Plant in Central Java alone produces up to 165 tons of silica sludge monthly, a volume comparable to waste generation in developed nations. This paradox of clean energy generation coupled with problematic waste forms the critical backdrop of this study. Rather than treating this byproduct as mere waste, recent research has redefined geothermal slag, containing 90–98% amorphous silica, as a valuable resource.[5,6] Its exceptional thermal stability, high surface area, and reactivity make it an ideal precursor for advanced materials.[5] Innovations have successfully converted into high-value products, including nanosilica, silica gels, components for lithium-

ion battery electrodes, and magnetic nanoparticles for separation technologies.[7,8] Among synthesis routes, the sol-gel method stands out as a promising low-temperature approach for producing high-purity silica.[9] It circumvents energy-intensive conventional processes while aligning with circular economy principles by valorising waste.[10,11] Nevertheless, conventional acid-catalysed sol-gel techniques (using HCl or H_2SO_4) face significant limitations. Rapid condensation kinetics often lead to uncontrolled pH fluctuations, resulting in inconsistent silica networks and heterogeneous particle morphologies.[11] Furthermore, the high corrosiveness of strong acids can damage equipment and introduce metallic impurities (e.g., Fe^{3+}, Zn^{2+}) from reactor walls, frequently compromising silica purity below 90%.[1,11] These drawbacks highlight a persistent trade-off between processing efficiency and product quality in traditional syntheses. To address these challenges, recent advancements have explored milder organic acids and novel heating methods. Citric acid has shown promise in sol-gel synthesis by acting as a chelating agent, stabilising the pH, and reducing metallic contamination; however, complete removal of organic residues remains a concern.[12] Concurrently, microwave-assisted processing has emerged as a superior alternative, enabling rapid and uniform heating that enhances reaction kinetics, improves particle uniformity, and offers finer control over the condensation environment.[13] This synergy of a benign chelating agent and efficient heating technology presents a compelling strategy to overcome historical limitations. This study therefore aligns with Sustainable Development Goals 9 (Industry, Innovation, and Infrastructure) and 12 (Responsible Consumption and Production) by proposing a sustainable waste-to-resource pathway. We aim to develop an optimised synthesis process for silica nanoparticles from geothermal slag using a citric acid-assisted sol-gel method coupled with microwave heating. The primary objective is to systematically investigate the effect of precise pH variations (1, 3, 5, 7, and 13) during condensation on the purity, yield, and morphological characteristics of the resulting silica nanoparticles. This comprehensive optimisation gap has not yet been fully addressed in the context of geothermal waste. By bridging this knowledge gap, our work seeks to contribute a scalable, efficient, and environmentally benign protocol for transforming geothermal waste into high-value nanomaterials, ultimately supporting both material science innovation and global sustainability objectives.

EXPERIMENTAL

Materials

Geothermal slag was sourced from the Dieng Power Plant operated by PT Geo Dipa Energi in Central Java, Indonesia. All chemicals used were of analytical grade: sodium hydroxide, citric acid, and methanol procured from Merck.

Extraction and Synthesis of Silica Nanoparticles

Silica nanoparticles were synthesized from geothermal slag using a citric acid-assisted sol-gel method, followed by microwave treatment. The process comprised three consecutive stages. First, in the alkaline extraction and silica sol formation stage, approximately 5.62 g of dried geothermal slag was dissolved in 75 mL of an aqueous NaOH solution (containing 7.5 g NaOH) at 100 °C under continuous stirring at 240 rpm for 3 hours. This step converted solid silica (SiO_2) into soluble sodium metasilicate (Na_2SiO_3) via the reaction.[14]

$$SiO_2(s) + 2NaOH(aq) \rightarrow Na_2SiO_3(aq) + H_2O(l) \quad (\Delta H = 136.4 \text{ kJ/mol}) \qquad (1)$$

The mixture was then centrifuged to remove any undissolved residue, yielding a clear sodium silicate filtrate, referred to as the silica sol. Subsequently, pH-controlled gelation was performed using citric acid titration. The silica sol was titrated under constant stirring with a 5 M citric acid solution to systematically achieve target pH values of 1, 3, 5, 7, and 13, where pH 13 served as an alkaline control. Gel formation occurred via acid-induced condensation of silicate species, as shown by the following reaction.[14]

$$3Na_2SiO_3(aq) + 2C_6H_8O_7(aq) \rightarrow 2Na_3C_6H_5O_7(s) + 3SiO_2(s) + 3H_2O(l) \quad (\Delta H = -320.7 \text{ kJ/mol}) \qquad (2)$$

Finally, the purification, drying, and thermal treatment stage was conducted. The formed silica gel was immediately washed by repeated centrifugation (4000 rpm, 10 minutes per cycle) with distilled water, followed by a 10% methanol solution until the supernatant reached neutral pH, thereby removing ionic and organic residues. The purified gel was then oven-dried at 110 °C overnight. The resulting xerogel was

gently ground into a fine powder and subjected to stepwise microwave heating from 200 °C to 900 °C, with a 5-minute hold at each temperature, to study the effects of thermal treatment on structural stabilisation.

Characterization Techniques

The chemical, structural, and morphological properties of both the raw geothermal slag and the synthesised silica samples were comprehensively characterised using a suite of analytical techniques. Elemental composition and silica (SiO_2) purity were determined via X-ray fluorescence (XRF) using a Malvern Panalytical Epsilon 4 spectrometer. Crystalline phase identification and confirmation of the amorphous nature of the silica were performed using X-ray diffraction (XRD) on a Panalytical X'Pert 3 diffractometer with Cu-Kα radiation (λ = 1.5406 Å), scanning over a 2θ range of 10° to 90°. To investigate the molecular structure and identify key functional groups, such as Si–O–Si and Si–OH, Fourier transform infrared spectroscopy (FTIR) was performed on a Bruker Invenio R spectrometer, with spectra recorded over 400–4000 cm^{-1}. Morphological analysis and particle size evaluation were conducted using field-emission scanning electron microscopy (FESEM) on a Thermo Scientific Quattro microscope. Particle size distributions were quantified from FESEM images using ImageJ. Additionally, the silica recovery efficiency for each pH condition was calculated based on a mass balance approach using the following equation:

$$\%\,Recovery = \left[\frac{M_2 \times (\%SiO_2)_2}{M_1 \times (\%SiO_2)_1}\right] \times 100\% \qquad (3)$$

Where M_1 and $(\%SiO_2)_1$ represent the mass and SiO_2 content (in per cent) of the initial geothermal slag, respectively, and M_2 and $(\%SiO_2)_2$ correspond to the mass and SiO_2 content of the final silica product obtained after the synthesis and drying processes.

RESULTS AND DISCUSSION

Effect of pH on Silica Purity and Recovery

The influence of pH during the citric acid-assisted gelation stage on the purity and recovery yield of silica was quantitatively evaluated using X-ray fluorescence (XRF). The results, summarised in Table-1, demonstrate a clear pH-dependent trend. The highest silica purity (97.494% SiO_2) was achieved at pH 3, followed closely by pH 1 (97.323%) and pH 5 (96.906%). This indicates the optimal efficacy of citric acid as a complexing agent in weak to moderately acidic conditions (pH 1–5), where it effectively sequesters metal impurities such as Fe, Zn, and Ca.[15,16] In contrast, the synthesis under alkaline conditions (pH 13) resulted in a significant reduction in purity to 84.257%, primarily due to increased contamination from Fe_2O_3(4.316%) and ZnO (6.797%). This decline can be attributed to decreased stability of metal-citrate complexes at high pH, leading to the precipitation of metal hydroxides that become trapped within the forming silica gel matrix.[17,18] The process successfully eliminated major impurities in the raw slag, notably chlorine (19.078%) and potassium oxide (3.031%), across all acidic-to-neutral pH treatments.

Table-1: XRF Characterisation of Synthesised SiO_2

Oksida	Raw	pH 1	pH 3	pH 5	pH 7	pH 13
	% wt	% wt	% wt	% wt	% wt	% wt
SiO_2	73.240	97.323	97.494	96.906	96.299	84.257
$P2O_5$	0.683	0.590	0.568	0.583	0.615	0.676
K_2O	3.031				0.127	0.756
CaO	1.336	0.268	0.257	0.237	0.262	0.636
Fe_2O_3	1.589			0.486	0.446	4.316
ZnO	0.126				0.646	6.797
PbO	0.137				0.206	0.756
Cl	19.078					

However, silica purity did not correlate directly with recovery efficiency. As calculated using Eqn.-3 and presented in Table-2, the highest recovery yield of 68.94% was obtained at pH 7, despite its slightly lower purity (96.299%). In contrast, the condition yielding the highest purity (pH 3) resulted in a significantly lower recovery of 27.21%. This inverse relationship suggests that while highly acidic conditions favour

impurity complexation, they may also lead to less efficient gel precipitation or increased material loss during subsequent washing and filtration steps.[19–21] The extremely low recovery at pH 13 (1.84%) underscores the incompatibility of strong alkaline conditions with efficient silica recovery in this citric acid-mediated process.

Table-2: Silica Recovery Efficiency at Various pH Conditions

Sample	Final weight (g)	Final SiO_2 (%)	Initial weight (g)	Initial SiO_2 (%)	Recovery (%)
pH 1	1.75	97.323	5.62	73.324	41.33
pH 3	1.15	97.494	5.62	73.324	27.21
pH 5	2.28	96.906	5.62	73.324	53.62
pH 7	2.95	96.299	5.62	73.324	68.94
pH 13	0.09	84.257	5.62	73.324	1.84

Structural and Molecular Evolution Analysed by FTIR and XRD

The molecular structural evolution of silica as a function of pH was investigated using FTIR spectroscopy, as shown in Fig.-1. The spectra revealed distinct pH-dependent features. A broad band around 3225 cm^{-1}, attributed to O–H stretching from both adsorbed water and silanol (Si–OH) groups, was most prominent at pH 1 and 3. It indicates the presence of a less condensed, hydroxyl-rich silica network under strong acidic conditions.[22] The intensity of the band at approximately 1682 cm^{-1}, associated with the bending vibration of Si–OH, peaked at pH 5 and 7, suggesting optimal silanol formation within this pH range. In contrast, the sample synthesised at pH 13 showed a significant reduction in these hydroxyl-related bands. Concurrently, it exhibited intensified peaks characteristic of the Si–O–Si asymmetric stretching (~1050 cm^{-1}), symmetric stretching (~790 cm^{-1}), and bending (~460 cm^{-1}) vibrations.[23,24] This spectral shift confirms that alkaline conditions promote greater silica polymerisation and cross-linking, resulting in a more condensed Si–O–Si network at the expense of surface silanol groups.[25]

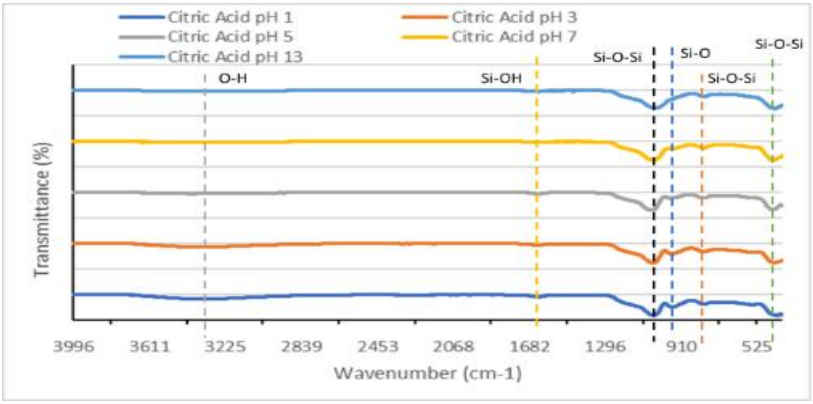

Fig.-1: FTIR Spectra of Silica Nanoparticles Synthesised from Geothermal Slag at Different pH Conditions

XRD analysis was employed to determine the crystallinity of the products. The diffraction patterns, presented in Fig.-2, confirmed the successful synthesis of amorphous silica across all pH conditions, as evidenced by the broad hump centred at $2\theta = 20–25°$ and the absence of sharp crystalline peaks.[26] The pattern for the raw geothermal slag showed distinct peaks corresponding to NaCl (COD 96-900-6375) and trace Fe (COD 96-901-3473) impurities. While the sol-gel process effectively removed the NaCl, the persistence of a minor Fe peak in some synthesised samples indicates that metallic impurities from the original slag can be challenging to eliminate through standard washing, underscoring the importance of the initial purification achieved by citric acid complexation.[27,28] The preserved amorphous nature is advantageous, as it typically confers higher surface area and reactivity compared to crystalline silica phases.

Morphological Characterisation via FESEM

The morphological impact of pH was clearly captured by FESEM, as shown in Fig.-3. Samples synthesised in the acidic to neutral range (pH 1-7) exhibited relatively uniform amorphous aggregates.

Energy-dispersive X-ray spectroscopy (EDS) coupled with FESEM identified carbon as the primary impurity in these samples, likely originating from residual organic compounds or undecomposed citric acid.[29,30] Notably, these pH conditions successfully prevented the incorporation of detectable levels of heavy metals (Na, Zn, Fe) into the silica particles.

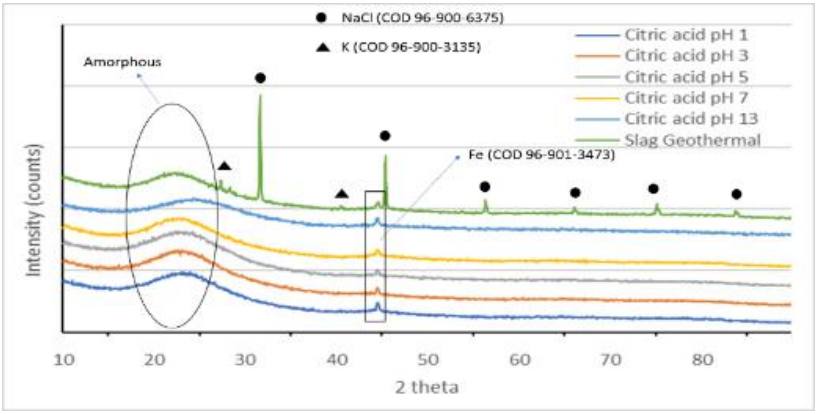

Fig.-2: XRD Patterns of Raw Geothermal Slag and Silica Nanoparticles Synthesised at Different pH Values

The sample at pH 7 showed a particularly well-developed and homogeneous network, consistent with the stronger Si–O–Si bonding observed in its FTIR spectrum.[31] Particle size distribution analysis, derived from ImageJ software, revealed that nanoparticles synthesised at pH levels of 5-7 had a narrower size distribution, ranging from 80 to 120 nm in diameter. In comparison, particles formed under stronger acidic conditions (pH 1-3) were larger and more aggregated, with sizes ranging from 150 to 300 nm. In stark contrast, the morphology of the silica produced at pH 13 was markedly different, exhibiting more defined spherical and floral-like structures. However, this improved morphological definition came at the cost of purity, as corroborated by XRF data. The alkaline environment facilitates different growth kinetics leading to these distinct shapes but also compromises the chelating efficiency of citric acid, allowing inorganic impurities to incorporate into the silica structure.

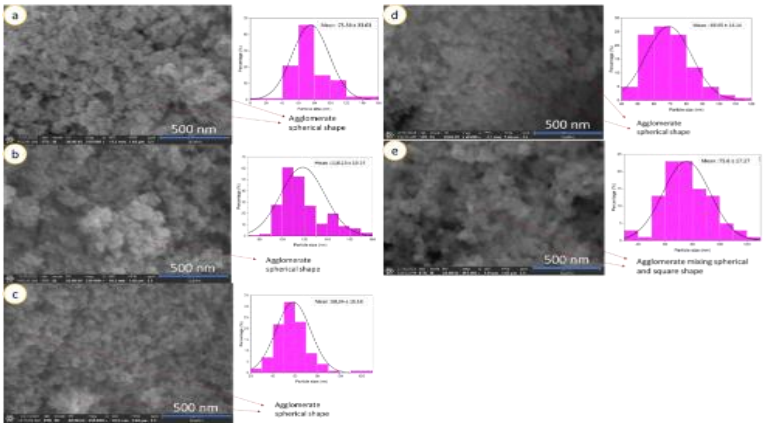

Fig.-3: FESEM Images Showing the Morphology of Silica Nanoparticles Synthesised at (a) pH 1, (b) pH 3, (c) pH 5, (d) pH 7, and (e) pH 13

Contextualising Findings and Contribution to SDGs

The results of this study clearly demonstrate that pH is a powerful and critical parameter for tailoring the properties of silica nanoparticles derived from geothermal waste. The finding that pH 3 maximises purity while pH 7 maximises recovery provides a practical roadmap for process optimisation, depending on the desired product specification, high-purity nanosilica for advanced applications, or higher yield for bulk material use. This work directly addresses Sustainable Development Goal 9 (Industry, Innovation, and Infrastructure) by innovating a waste-to-resource technology that adds value to an industrial byproduct.

Furthermore, it contributes to SDG-12 (Responsible Consumption and Production) by advancing the principles of a circular economy, wherein waste from clean energy production is sustainably upcycled into a functional nanomaterial. By replacing conventional strong acids with a milder chelating agent and employing energy-efficient microwave heating, this research also aligns with greener chemical synthesis pathways. The insights gained into the pH-dependent mechanisms of impurity complexation, condensation, and particle growth significantly enrich the existing body of knowledge on sol-gel chemistry applied to complex, real-world waste streams, offering a replicable framework for the valorisation of similar silica-rich wastes.

CONCLUSION

This study demonstrates that pH plays a critical role in controlling the synthesis of silica nanoparticles from geothermal slag using a citric acid-assisted sol-gel process. The highest purity (97.494% SiO_2) was achieved at pH 3, while the maximum recovery (68.94%) occurred at pH 7, producing nanoparticles with a uniform size distribution of 80–120 nm. Alkaline conditions (pH 13) promoted silica polymerisation but introduced significant metal impurities, resulting in a purity of 84.257%. Structural analyses confirmed the amorphous nature of all synthesised silica and revealed pH-dependent evolution from silanol-rich networks to condensed Si–O–Si structures. These results provide a clear scientific basis for optimising silica production from industrial waste, enabling the selection of materials based on purity or yield requirements. This work advances sustainable nanomaterial synthesis and directly contributes to SDG 9 (Industry, Innovation, and Infrastructure) and SDG 12 (Responsible Consumption and Production) by promoting circular-economy principles through the valorisation of geothermal byproducts.

ACKNOWLEDGMENTS

The authors acknowledge the facilities, scientific and technical support from the Minerals Laboratory Lampung, National Research and Innovation Agency, through E-Layanan Sains, Badan Riset dan Inovasi Nasional (BRIN). This research is also supported by the Research Organisation for Nanotechnology and Materials, BRIN, through the Rumah program funding research and RIIM 7. We also thank you for the support from the Department of Physics, Faculty of Mathematics and Natural Sciences, Universitas Indonesia.

CONFLICT OF INTERESTS

The authors declare that there is no conflict of interest.

AUTHOR CONTRIBUTIONS

The present work is related to *SDG-12: Responsible Consumption and Production*. All the authors contributed significantly to this manuscript, participated in reviewing/editing and approved the final draft for publication. The research profile of the authors can be verified from their ORCID ids, given below:

D.C. Birawidha http://orchid.org/0000-0001-8279-7401
A. Manaf http://orchid.org/0000-0002-6142-3918
W. Astuti https://orcid.org/0000-0001-9364-4291
A. Daulay http://orchid.org/0000-0002-9046-0750
H.T.B.M. Petrus https://orcid.org/0000-0001-9372-0784
U. Dani http://orchid.org/0009-0006-9599-2170
S. Widayati http://orchid.org/0000-0003-0201-6658

Cite this article as: D. C. Birawidha *et al.*, *Rasayan J. Chem.*, 19(1), 525-532(2026), https://doi.org/10.317 88/RJC.2026.1919473.

REFERENCES

1. V. S. H. Sujoto, I. W. C. W. H. Tangkas, W. Astuti, S. Sumardi, S. N. A. Jenie, A. P. C. Tampubolon,

S. Syamsumin, A. P. Utama, H. T. B. M. Petrus, Y. Kusumastuti, *Jurnal Rekayasa Proses,* **2,** 17(2023), https://doi.org/10.22146/jrekpros.77696
2. F. H. Ouerghi, M. Omri, K. S. Nisar, R. M. Abd El-Aziz, A. I. Taloba, *Alexandria Engineering Journal,* ***97***, 215(2024), https://doi.org/10.1016/j.aej.2024.03.094
3. B. Sinaga, S. Tobing, *Preprints,* 2024061896(2024), https://doi.org/10.20944/preprints202406.1896.v1
4. H. Widiyandari, P. Pardoyo, J. Sartika, O. A. Putra, A. Purwanto, L. Ernawati, *International Journal of Engineering, Transactions A: Basics,* **34**, 7(2021), https://doi.org/10.5829/IJE.2021.34.07A.02
5. S. N. A. Jenie, A. Ghaisani, Y. P. Ningrum, A. Kristiani, F. Aulia, H. T. M. B. Petrus, In *AIP Conference Proceedings*, **2026**, 02008(2018), https://doi.org/10.1063/1.5064968
6. H. T. B. M. Petrus, M. Olvianas, M. F. Shafiyurrahman, I. G. A. A. N. Pratama, S. N. A. Jenie, W. Astuti, M. I. Nurpratama, J. J. Ekaputri, F. Anggara, *Gels,* **8,** 4(2022**)**, https://doi.org/10.3390/gels8040233
7. A. R. Adiatama, R. F. Susanti, W. Astuti, H. Petrus, K. C. Wanta, *Metalurgi,* **37(2)**, 73(2022)
8. W. A. Fitri, L. Sururoh, S. N. A. Jenie, In *Proceedings Of The 5th International Symposium On Applied Chemistry*, **2175**, 020080(2019), https://doi.org/10.1063/1.5134644
9. D. C. Birawidha, A. Manaf, W. Astuti, A. Daulay, H. Petrus, N. A. Ningrum, D. Asmi, M. K. Nariswari, *Periodica Polytechnica Chemical Engineering.* **4**, 69(**2025)**, https://doi.org/10.3311/PPch.41906
10. X. Jiang, X. Tang, L. Tang, B. Zhang, H. Mao, *Ceramics International,* **6**, 45(2019**)**, https://doi.org/10.1016/j.ceramint.2019.01.067
11. N. N. Maseko, D. Enke, S. A. Iwarere, O. S. Oluwafemi, J. Pocock, *Sustainability,* **15,** 4626(2023**)**, https://doi.org/10.3390/su15054626
12. A. N. Amenaghawon, J. E. Ayere, U. O. Amune, I. C. Otuya, E. C. Abuga, C. L. Anyalewechi, O. V. Okoro, J. A. Okolie, P. K. Oyefolu, S. O. Eshiemogie, *Environmental Research,* **251**, 118703(2024), https://doi.org/10.1016/j.envres.2024.118703
13. D. C. Freitas, O. Mazali, A. Sigoli, S. Francischini, M. Aur, Z. Arruda, *The Royal Society of Chemistry,* **13,** 2023, https://doi.org/10.1039/d3ra05648a
14. A. Daulay, Andriayani, Marpongahtun, S. Gea, Tamrin, *Rasayan Journal of Chemistry,***14**, 3(2021), http://doi.org/10.31788/RJC.2021.1436351
15. R. S. Azis, S. Sulaiman, I. R. Ibrahim, A. Zakaria, J. Hassan, N. N. C. Muda, R. Nazlan, N. M. Saiden, Y. W. Fen, M. S. Mustaffa, K. A. Matori, *Nanoscale Research Letters,* **13**, Article 160(2018**)**, https://doi.org/10.1186/s11671-018-2562-x
16. E. Książek, *Molecules,* **1**, 29(2024), https://doi.org/10.3390/molecules29010022
17. M. Zabiszak, M. Nowak, K. Taras-Goslinska, M. T. Kaczmarek, Z. Hnatejko, R. Jastrzab, *Journal of Inorganic Biochemistr*y, **182**, 37(2018), https://doi.org/10.1016/j.jinorgbio.2018.01.017
18. A. E. Danks, S. R. Hall, Z. Schnepp, *Materials Horizons,* **2**, 3(2026)
19. E. H. Sabino, M. R. Derolf, J. L. Bass, *Advances in X-Ray Analysis,* **1983**, 487(2019**)**, https://doi.org/10.1154/S0376030800017432
20. R. A. Sazali, K. S. Sorbie, L. S. Boak, N. S. Al Badri, H. Veny, F. H. Hamid, M. Z. Z. Abidin, *Bulletin of Chemical Reaction Engineering & Catalysis,* **3**, 17(2022), https://doi.org/10.9767/bcrec.17.3.15290.661-682
21. M. Mehri, N. Fallah, B. Nasernejad, *npj Clean Water,* **4,** 1(2021), https://doi.org/10.1038/s41545-021-00135-0
22. R. Ellerbrock, M. Stein, J. Schaller, *Scientific Reports,* **1**, 12(2022), https://doi.org/10.1038/s41598-022-15882-4
23. C. Collantes, V. González Pedro, M. J. Bañuls, A. Maquieira, *ACS Applied Nano Materials,* **2,** 4(2021), https://doi.org/10.1021/acsanm.0c03340
24. D. S. Volkov, O. B. Rogova, M. A. Proskurnin, *Agronomy,* **11**, 9(2021), https://doi.org/10.3390/agronomy11091879
25. F. Koç, S. S. Çok, N. Gizli, *Engineering Structure and Materials,* **6**, 257(2020), https://doi.org/10.17515/resm2019.166ma1203

26. O. G. M. Sandoval, G. C. D. Trujillo, A. E. L. Orozco, *Water Resources and Industry,* **20,** 15(2018), https://doi.org/10.1016/j.wri.2018.07.002
27. Y. Kusumastuti, H. T. B. M. Petrus, F. Yohana, A. T. Buwono, R. B. Zaqina, In *AIP Conference Proceedings*, **1823**, 020127(2017), https://doi.org/10.1063/1.4978200
28. P. P. Nayak, S. Nandi, K. Bhunia, A. K. Datta, *Material Chemistry and Physics,* **293,** 126944(2023), https://doi.org/10.1016/j.matchemphys.2022.126944
29. Andriayani, Marpongahtun, Suharman, A. Daulay, *Case Studies in Chemical and Environmental Engineering,* **7**, 100287(2023), https://doi.org/10.1016/j.cscee.2022.100287
30. K. S. Naidu, N. Annapurna, R. S. K. Sharma, G. V. S. Prasad, M. R. Kumar, V. Anita, *Rasayan Journal of Chemistry,* **4,** 18*(*2025), http://doi.org/10.31788/RJC.2025.1849389
31. S. Xu , L. Zhao , S. Hua , M. Che , J, Hou , Y. Liu , H. Cao , J. Zhang, *Applied Surface Science,* **726,** 165913 (2026), https://doi.org/10.1016/j.apsusc.2026.165913

[RJC-9473/2025]